Operation of quantum phase gate using neutral atoms in microscopic dipole trap

Igor E. Protsenko, Georges Reymond, Nicolas Schlosser, Philippe Grangier

Operation of a quantum phase gate using neutral atoms in microscopic dipole traps

I. E. Protsenko,[1,2,3] G. Reymond,[1] N. Schlosser,[1] and P. Grangier[1,*]
[1]*Laboratoire Charles Fabry de l'Institut d'Optique, UMR 8501 du CNRS, F91403 Orsay, France*
[2]*Lebedev Physics Institute, Leninsky Prospect 53, Moscow, Russia*
[3]*Scientific Center of Applied Research, JINR, Dubna, Russia*
(Received 25 September 2001; published 15 April 2002)

In this paper we propose and analyze various operating regimes of a quantum phase gate built on two atoms trapped in two independent dipole traps. The gate operates when the atoms are excited using a two-photon transition from the hyperfine manifold of ground states up to Rydberg states with strong dipole-dipole interaction. Experimental requirements are discussed to reach a fast (microsecond) gate operation.

DOI: 10.1103/PhysRevA.65.052301 PACS number(s): 03.67.Lx, 32.80.Pj, 32.80.Rm, 34.60.+z

I. INTRODUCTION

The manipulation of individual quantum objects, such as atoms, ions, or photons, opens the way to controlled engineering of a quantum state of small sets of trapped particles, in order to encode and process information at the quantum level. Recent achievements in this direction use either trapped ions [1–3] or trapped photons in cavity QED systems [3,4]. A third possibility, which has been actively studied theoretically [5,6], is to use trapped neutral atoms. From the experimental side, we have demonstrated recently that it is possible to load and detect individual atoms in an optical dipole trap with a submicrometer size [7]. Due to the extremely small trapping volume, only one atom can be loaded at a time, resulting in strongly sub-Poissonnian statistics of the number N of atoms in the trap. Moreover, by sending another trapping beam at a small angle in the same optics, we have trapped two atoms at a controlled distance, which can be adjusted in the range $1-10$ μm (see Fig. 1). The dipole trap is initially loaded from a very low density magneto-optical trap (MOT), which cools the atoms and allows us to detect them easily from the induced fluorescence. The presence of one atom in the trap can be detected within less than 1 ms, and then by turning off the MOT the atom can be kept in the trap for several seconds, with a very low fluorescence rate. This setup opens possibilities to explore various proposed schemes for atom-atom entanglement, such as controlled cold collisions [8] or atomic dipole-dipole coupling [9].

In this paper we will investigate more quantitatively several schemes derived from the fast quantum phase gate that has been proposed in Ref. [10]. In this proposal, the qubits are implemented by using hyperfine sublevels of the atomic ground state [5,6,11], and rotations in the one-qubit subspace are achieved by inducing Raman transitions between these sublevels, separated by $\omega_F/2\pi = 6.83$ GHz for ^{87}Rb. Fast (microsecond) operation can be achieved by using the trapping laser itself as Raman beams, together with a pulsed control beam, addressing each atom, and detuned from the trapping beam by ω_F [12]. For two-qubit operations, one can selectively couple one of the hyperfine sublevels to a high-n Rydberg state by using a direct two-photon transition involving a pulsed blue laser and the trapping beam. Analyzing the operation of such a quantum gate requires first to study the dipole-dipole interaction in Rydberg states, which is the basic physical mechanism for atom-atom coupling, as well as the multiphoton absorption in a time-dependent laser field, which is required to reach Rydberg states. We will also pay attention to limiting factors related to the limited lifetime of Rydberg states, and to the deleterious effects of thermal photon absorption, photoionization, and interatomic distance fluctuations. These problems will be treated using several approximations in order to obtain analytical results whenever possible. The relevant parameters values, such as laser frequencies, powers, interatomic distances, will be chosen to match what is accessible experimentally [7]. The Rydberg state evaluations will be carried out using spectroscopic data and formulas found in the literature.

The paper is organized as follows. In Sec. II we recall the general definition of a quantum phase gate and we describe how it might be implemented in our setup [7]. Section III introduces some expressions, approximations, and numerical parameters used in the paper and studies one-atom operations. In Sec. IV we examine the dipole-dipole interaction for Rydberg states, which is the basic ingredient for the two-qubit gate operations. Section V contains the main results of the paper and is subdivided into three sections. In Sec. V A, the general equations for the two-atom operations are derived and then simplified for two cases of particular interest. In the first case, the resonant excitation is possible for one atom only, while the simultaneous excitation of two atoms is suppressed due to the dipole-dipole interaction. In the second case, the two atoms can be excited together only, while the one-atom excitation is nonresonant. The first case is analyzed in greater detail in Sec. V B for a ''square pulse'' shape of the exciting laser field. The advantage of this case is in the low sensitivity to fluctuations in the interatomic distance. The second case is analyzed in Sec. V C, it leads to a specific ''self-transparency'' regime of the interaction of two atoms with the field. The sensitivity of this regime to small fluctuations in the interatomic distance is discussed. A final discussion about advantages and disadvantages of each regime, and experimental perspectives, is presented in Sec. VI.

*Corresponding author. Email address: philippe.grangier@iota.u-psud.fr

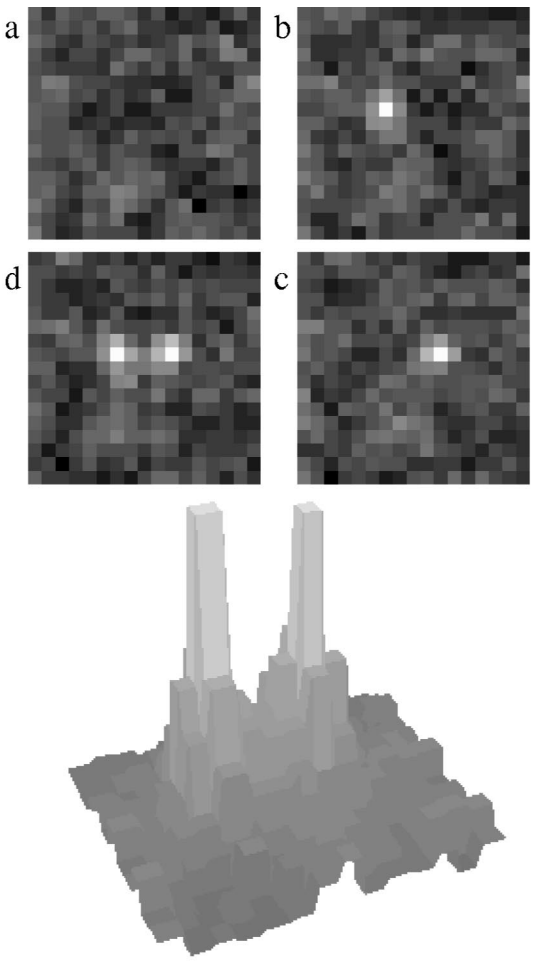

FIG. 1. Fluorescence signals from atoms trapped into two neighboring independent dipole traps. The fluorescence is induced by ''optical molasses'' beams that are always switched on to take the pictures. Each square is a pixel of the charge coupled device camera and corresponds to a size of 1 μm in the atom's space. The top picture shows two-dimensional (2D) images corresponding to no atom (a), one (left or right) atom (b),(c), and two atoms in the traps (d). The bottom picture shows a 3D reconstruction of the fluorescence signal from two trapped atoms. Dark regions correspond to lower fluorescence signal.

II. FORMULATION OF THE PROBLEM

In this section we recall the definition of a quantum phase gate and present a possible implementation of such a gate using two ^{87}Rb atoms trapped in two separate dipole traps.

A quantum computer, described by the wave function $|\Psi\rangle=\Sigma_{k=1}^{n}A_k|k\rangle$, carries out a unitary transformation in the Hilbert space of its states $|k\rangle$ and transforms the initial state vector $\{A_1^{in},\ldots,A_n^{in}\}$, which contains the initial data, to the final state vector $\{A_1^{out},\ldots,A_n^{out}\}$, which contains the result. Any computer is a combination of many ''universal logical elements,'' and, in principle, a quantum computer can be built from only two different kinds of elements: the conditional quantum phase gate acting on two qubits and the arbitrary rotation gate acting on one qubit. With these gates one can construct an arbitrary unitary $n\times n$ matrix [13,14]. Taking some states $|g\rangle$, $|e\rangle$ of an atom as the qubit states, the single-qubit rotation can be easily obtained by inducing Rabi oscillations in the $|g\rangle\rightarrow|e\rangle$ transition. Thus, an important problem for implementing a quantum computer is designing a conditional quantum phase gate, which transforms the two-qubit state $|a\rangle|b\rangle$ according to [4],

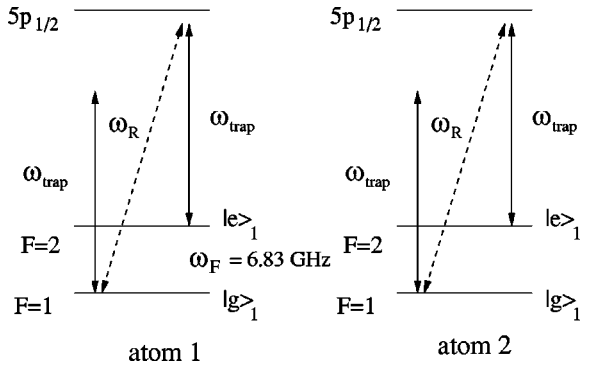

FIG. 2. Preparation of the initial states of Rb atoms using one-qubit rotations. It is assumed that the Raman transitions can be driven independently for each atom.

$$|a\rangle|b\rangle\rightarrow\exp(i\varphi\delta_{a,g}\delta_{b,g})|a\rangle|b\rangle, \tag{1}$$

where $|a\rangle$, $|b\rangle$ stand for the basis states $|e\rangle$ or $|g\rangle$ of two qubits and $\delta_{b,g}$, $\delta_{a,g}$ are Kronecker symbols.

Here the two qubits will be encoded on the ground hyperfine sublevels of two ^{87}Rb atoms trapped in two separate optical dipole traps. We assume that for each atom ($k=1,2$), Raman transitions between the upper state $|e\rangle_k(F=2)$ and the lower state $|g\rangle_k$ $(F=1)$ of the hyperfine manifold of the lowest $5S_{1/2}$ state can be driven independently with the help of additional fields of frequencies ω_R, which are detuned from the trapping field frequency ω_{trap} by $\omega_R-\omega_{trap}=\omega_F$ [12], as shown in Fig. 2. This provides one-qubit rotations. Our goal is then to obtain a fast operation of the conditional quantum gate transformation (1), which can be realized under the experimental conditions of [7]. With respect to previous proposals [5,6,15], we avoid the need of keeping atoms in highly excited Rydberg states as well as the fine level tuning using a constant electric field. However, it will appear that compromises are necessary anyway, and different possibilities each with some advantages and disadvantages will be examined.

The transformation (1) can be performed in two steps. The first step involves a *two-atom operation*. The atoms in states $|g\rangle_k$ are excited to Rydberg states using a light pulse and then driven back to states $|g\rangle_k$ with some phase shift. While the atoms are in the Rydberg states, they are strongly coupled through a dipole-dipole (d-d) interaction. The atoms in $|e\rangle_k$ state are not excited and are, therefore, not affected by d-d interaction. After this the two-atom operation step in the state evolution is

$$|a\rangle|b\rangle\rightarrow\exp(-i\varphi_0\delta_{a,g}-i\varphi_0\delta_{b,g}+i\varphi\delta_{a,g}\delta_{b,g})|a\rangle|b\rangle. \tag{2}$$

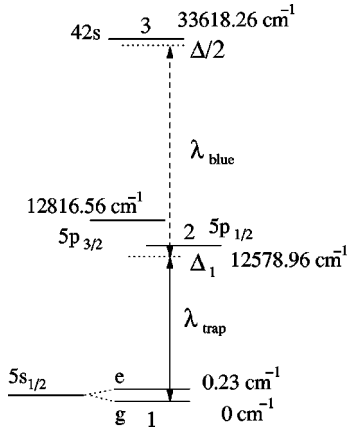

FIG. 3. Two-photon transitions to the Rydberg state of the ^{87}Rb atom.

The second step is a *one-atom operation*, which changes the phase of the single-atom state $|g\rangle_k$ in the absence of *d-d* interaction between atoms, and does nothing with the state $|e\rangle_k$, so that

$$|a\rangle|b\rangle \rightarrow \exp(i\varphi_0\delta_{a,g}+i\varphi_0\delta_{b,g})|a\rangle|b\rangle. \tag{3}$$

The purpose of the two-atom operation is to create the conditional (state-dependent) phase shift required by Eq. (1), while the one-atom operation will compensate unwanted phase offsets φ_0, which occur at the two-atom stage. Though there may be simpler ways to obtain single-atom phase shifts, for the uniformity of theoretical and experimental treatment all these operations will be obtained from the transient excitation of (the same) Rydberg states. We first describe one-atom operations, which are easier to implement.

III. ONE-ATOM OPERATIONS

Here we estimate the values of various parameters that are necessary for the realization of the one-atom operations (3) in our experimental conditions. Similar parameter values will be utilized in the rest of the paper.

The operations (3) can be carried out by the interaction of atoms with a pulse of light, which is close to resonance with the transition between $|g\rangle$ and some excited state, but much further away from resonance with any transition from the $|e\rangle$ state. The last condition can be easily satisfied because of the large difference in energies between the $|e\rangle$ and $|g\rangle$ states, $\omega_F/2\pi=6.83$ GHz. For all numerical calculations we will use the two-photon transition $|g\rangle_k \rightarrow |5p_{1/2}\rangle_k \rightarrow |42s\rangle_k$ shown in Fig. 3, but other choices may be possible [16].

The two-photon transition can be described using an ''effective'' coupling field $\mathcal{E}(t)=\frac{1}{2}[\Omega_2(t)e^{i\omega t}+\text{c.c.}]$, where $\omega=\omega_0-\Delta/2$, ω_0 is the $|g\rangle_k \rightarrow |42s\rangle$ transition frequency for a single atom in free space, $\Delta/2$ is the detuning from the two-photon resonance, and $\Omega_2(t)$ is the two-photon Rabi frequency. One of two fields participating in the transition is the optical dipole trap field of $\lambda_{trap}=802.3$ nm interacting with the $|5s\rangle \rightarrow |5p_{1/2}\rangle$ transition (it is assumed that other transitions from the $|5s\rangle$ state are further off-resonance and can be neglected). The amplitude of the trapping field is constant in time. The time-varying field is a pulse of ''blue'' light that can be obtained either from a pulsed tunable laser or by ''chopping a slice'' from a continuous laser using a fast modulator. Numerical calculations will be done with $\lambda_{blue}=472.7$ nm (argon ion laser line), interacting with the $|5p_{1/2}\rangle \rightarrow |42s\rangle$ transition. It is to be noticed that the blue light excitation is applied simultaneously on both atoms. Therefore tight focusing is not required and the ''blue'' beam waist may be larger than the interatomic distance. The two-photon transition $|5s\rangle \rightarrow |42s\rangle$ is analyzed in Appendix I, and the two-photon Rabi frequency is

$$\Omega_2(t)=\frac{\Omega_{trap}\Omega_{blue}(t)}{2\Delta_1}, \tag{4}$$

where Ω_{trap} and $\Omega_{blue}(t)$ are the Rabi frequencies of the trap and the blue fields, respectively, and Δ_1 is the detuning from the one-photon resonance in the $|5s\rangle \rightarrow |5p_{1/2}\rangle$ transition. For single-atom operations we assume that $\Omega_2(t)/\Delta \ll 1$ and everywhere below, $\Delta \ll \omega_F$, so that we can neglect the population of the $|42s\rangle$ state and the interaction of the field $\mathcal{E}(t)$ with atoms in the state $|e\rangle_k$. As long as the duration of the pulse τ is much shorter than the spontaneous emission lifetime $\tau_{sp}^{(42s)}$ of the $|42s\rangle$ state, the time evolution of the $|g\rangle_k$ state is simply a phase shift that can be written as

$$|g\rangle_k \exp\left(\frac{i}{4}\int_0^t \Omega_4(t')dt'\right), \quad \text{where} \quad \Omega_4(t)\equiv\frac{2\Omega_2^2(t)}{\Delta}. \tag{5}$$

This evolution performs operations (3) with

$$\varphi_0=\frac{1}{4}\int_0^t \Omega_4(t')dt'. \tag{6}$$

Let us estimate the values of parameters necessary to satisfy $\tau \ll \tau_{sp}^{(42s)}$. The oscillator strength for the $|5s\rangle \rightarrow |5p_{1/2}\rangle$ transition is $f_{5s\text{-}5p}\approx 1/3$ and we calculated the oscillator strength for the $|5p_{1/2}\rangle \rightarrow |42s\rangle$ transition to be $f_{5p\text{-}42s}\approx(5/3)\times 10^{-6}$ (see Appendix B). Let us suppose that the blue field is a ''square pulse'' so that Ω_{blue} is constant in the time interval τ. Taking the cross section and the power for the trap and blue beams as $S_{trap}=10^{-8}$ cm^2, $P_{trap}=10$ mW and $S_{blue}=10^{-6}$ cm^2, $P_{blue}=0.5$ W, respectively, we estimate $\Omega_{trap}\sim 5\times 10^{11}$ s^{-1} and $\Omega_{blue}\sim 10^9$ s^{-1}. Supposing $\varphi_0 \sim \pi$ and taking $\Delta=10^9$ s^{-1} [so that $2\Omega_2(t)/\Delta=0.1\ll 1$], we obtain that the duration of the pulse carrying out the transformation (3) is $\tau\approx 10$ μs. This value is indeed significantly shorter than $\tau_{sp}^{42s}\approx 120$ μs, which is our estimation for the spontaneous emission time of the 42*s* state. We point out that thermal photons may reduce significantly the effective lifetime of the Rydberg states, and we assume that appropriate cooling and/or shielding is used to eliminate them, though this may be a significant practical problem [19]. In Appendix C we also show that the probability for the Rydberg state to be photoionized by the strong trapping field can be kept reasonably small. Therefore, apart from the influence of thermal photons, the conditions for the one-atom operations can be easily satisfied in the experiment.

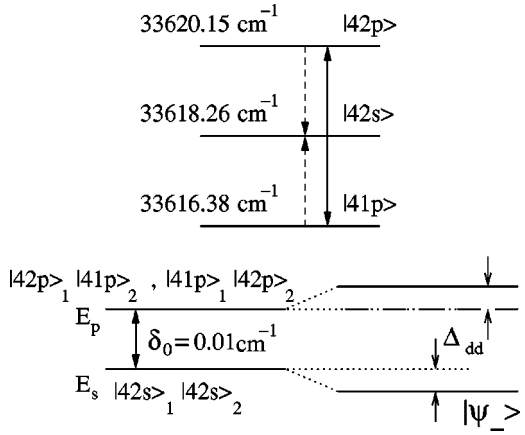

FIG. 4. Rydberg states of single ^{87}Rb atom (top) and two-atom states (bottom).

IV. DIPOLE-DIPOLE INTERACTION BETWEEN RYDBERG STATES

In order to proceed with the analysis of the two-atom operations we have to determine the states of two atoms spatially separated by a few microns, when the atoms are excited to Rydberg states and coupled by a strong *d-d* interaction. Let us consider the $|41p\rangle$, $|42s\rangle$, and $|42p\rangle$ states of ^{87}Rb atom shown in the top part of Fig. 4. For simplicity we do not distinguish the fine and the hyperfine structures of Rydberg states, though the fine-structure splitting of the $42p$ state is ≈ 0.047 cm^{-1} [17], and it should be taken into account for more precise calculations. In the numerical evaluations we use the average weighted energies of Rydberg states presented in [18].

Since the transitions $|41p\rangle \rightarrow |42s\rangle$ and $|42s\rangle \rightarrow |42p\rangle$ are nearly resonant, the two-atom states $|42s\rangle_1|42s\rangle_2$ are coupled to the states $|41p\rangle_1|42p\rangle_2$ and $|42p\rangle_1|41p\rangle_2$ due to the resonant *d-d* interaction, which mixes these bare states and leads to new two-atom states. Let us find the coupled states in terms of atom eigenstates without *d-d* interaction. We introduce a coordinate system with axis *z* directed from atom 1 to atom 2. Following the approach of [20] we consider the $|n,p,\alpha\rangle$ basic states, $\alpha=x,y,z$, which correspond to the dipole momentum of atom transitions directed along *x*, *y*, and *z* axes. Such states are linear combinations of usual states with magnetic quantum numbers $m=0,\pm 1$. The general expression for the wave function of a two-atom state is

$$|\psi\rangle = A_s|42s\rangle_1|42s\rangle_2 + \sum_{\alpha,\beta=x,y,z} A_{\alpha,\beta}|41p,\alpha\rangle_1|42p,\beta\rangle_2 + \sum_{\alpha,\beta=x,y,z} B_{\alpha,\beta}|42p,\alpha\rangle_1|41p,\beta\rangle_2. \quad (7)$$

In Eq. (7) there are 18 two-atom *p* states and one *s* state. The *s* state $|42s\rangle_1|42s\rangle_2$ always interacts with *p* states, so that there are no nonshifted states with the energy E_s. On the other hand, most of the *p* states do not participate in the *d-d* interaction and have the energy E_p, while some of them are shifted due to the *d-d* interaction (see the bottom part of Fig. 4). For atoms in $|np,\alpha\rangle$ and $|n'p,\alpha'\rangle$ states with $\alpha \neq \alpha'$ the dipole momenta of $ns \rightarrow n'p$ transitions are perpendicular to each other. There are 12 such states, they are not shifted and have energy E_p. For describing the other states it is convenient to define

$$|\psi_s\rangle = |42s\rangle_1|42s\rangle_2, \quad (8)$$

$$|\chi_\alpha\rangle = (1/\sqrt{2})(|41p,\alpha\rangle_1|42p,\alpha\rangle_2 - |41p,\alpha\rangle_2|42p,\alpha\rangle_1), \quad (9)$$

$$|\psi_\alpha\rangle = (1/\sqrt{2})(|41p,\alpha\rangle_1|42p,\alpha\rangle_2 + |41p,\alpha\rangle_2|42p,\alpha\rangle_1), \quad (10)$$

where $\alpha=x,y,z$. The dipole momenta of transitions from $|42s\rangle_1|42s\rangle_2$ to $|41p,\alpha\rangle_1|42p,\alpha\rangle_2$ and to $|41p,\alpha\rangle_2|42p,\alpha\rangle_1$ states have opposite phases, so that the three antisymmetric states $|\chi_\alpha\rangle$ are "dark states." Among other states, it is easy to check that the vector $(1/\sqrt{2})(|\psi_x\rangle - |\psi_y\rangle)$ is also uncoupled, because of the symmetry of *d-d* interaction with respect to the rotations of the coordinate system around axis *z*. Finally the general expression of the coupled states is

$$|\tilde{\psi}\rangle = A_s|\psi_s\rangle + A_z|\psi_z\rangle + A_\perp|\psi_\perp\rangle, \quad (11)$$

where $|\psi_\perp\rangle = (1/\sqrt{2})(|\psi_x\rangle + |\psi_y\rangle)$.

The Hamiltonian of the two-atom system is $H=H_0+V_{d\text{-}d}$, where H_0 is the energy operator in the absence of *d-d* interaction, with the diagonal matrix elements $E_s=\langle\psi_s|H_0|\psi_s\rangle = 67\,236.52$ cm^{-1} and $E_p=\langle\psi_\alpha|H_0|\psi_\alpha\rangle = 67\,236.53$ cm^{-1}. The operator $V_{d\text{-}d}$ describes the *d-d* interaction. Since the resonant wavelength $\lambda \approx 0.5$ cm for the transitions between the Rydberg states is much larger than the typical distance between the two atoms, one can consider a static *d-d* interaction with the energy

$$V_{d\text{-}d} = \frac{\vec{\mu}_1 \cdot \vec{\mu}_2}{r^3} - 3\frac{(\vec{\mu}_1 \cdot \vec{r})(\vec{\mu}_2 \cdot \vec{r})}{r^5}, \quad (12)$$

where $\vec{\mu}_k = \{\hat{\mu}_{xk}, \hat{\mu}_{yk}, \hat{\mu}_{zk}\}$ is the operator of the dipole momentum of the transition of atom $k=1,2$ and $\vec{r}$ is the radius vector from atom 1 to atom 2. The nonzero matrix elements of $V_{d\text{-}d}$ are thus

$$\langle\psi_{x,y}|V_{d\text{-}d}|\psi_s\rangle = \langle\psi_s|V_{d\text{-}d}|\psi_{x,y}\rangle^* = \sqrt{2}\hbar\Gamma_{d\text{-}d},$$

$$\langle\psi_z|V_{d\text{-}d}|\psi_s\rangle = \langle\psi_s|V_{d\text{-}d}|\psi_z\rangle^* = -2\sqrt{2}\hbar\Gamma_{d\text{-}d},$$

$$\langle\psi_\perp|V_{d\text{-}d}|\psi_s\rangle = \langle\psi_s|V_{d\text{-}d}|\psi_\perp\rangle^* = 2\hbar\Gamma_{d\text{-}d},$$

where $\hbar\Gamma_{d\text{-}d} = \mu_{41}\mu_{42}/r^3$, $\mu_{41} = \langle 41p,\alpha|_k\hat{\mu}_{\alpha k}|42s,\alpha\rangle_k$, $\mu_{42} = \langle 42p,\alpha|_k\hat{\mu}_{\alpha k}|42s,\alpha\rangle_k$ for $k=1,2$. One can then find three eigenstates for *H*,

$$|\psi_p\rangle = \sqrt{2/3}[|\psi_\perp\rangle + (1/\sqrt{2})|\psi_z\rangle] \tag{13}$$

and

$$|\psi_\pm\rangle = \alpha_\pm[|\psi_s\rangle \mp \xi_\pm(\sqrt{2}|\psi_z\rangle - |\psi_\perp\rangle)], \tag{14}$$

where

$$\xi_- = 2\Gamma^*_{d\text{-}d}/[\delta_0(1+\theta)], \quad \xi_+ = 2\Gamma^*_{d\text{-}d}/(\delta_0\theta),$$

$$\alpha_\pm = [1+3|\xi_\pm|^2]^{-1/2}$$

and

$$\theta = (1/2)[\sqrt{1+48(|\Gamma_{d\text{-}d}|/\delta_0)^2} - 1]. \tag{15}$$

The state $|\psi_p\rangle$ has energy E_p and the states $|\psi_\pm\rangle$ have, respectively, energies $E_+ = E_p + \hbar\Delta_{d\text{-}d}$ and $E_- = E_s - \hbar\Delta_{d\text{-}d}$ where $\Delta_{d\text{-}d} = \delta_0\theta$ and $\hbar\delta_0 = E_p - E_s = 0.01$ cm^{-1}. These states are well separated, because $\Delta_{d\text{-}d} > 1.2\times 10^7$ s^{-1} for the typical interatomic distance $r < 5$ μm (see Fig. 4), which is much larger than the Rydberg state lifetime. It can also be seen easily that for $r \geqslant 1$ μm the admixture of $|\psi_s\rangle$ in $|\psi_-\rangle$ is much bigger that in $|\psi_+\rangle$, and thus the two-photon transition to the Rydberg states, which occurs through $|\psi_s\rangle$, is maximum for the $|\psi_-\rangle$ state. Since this state with energy E_- is also well separated from the other ones, we will consider below that only $|\psi_-\rangle$ is involved in the interaction of atoms with the two-photon field. This state is essentially the initial nondegenerate two-atom state $|\psi_s\rangle$ down-shifted by the *d-d* interaction (see Fig. 4).

In the calculations above we neglected the retardation in the *d-d* interaction. In a first approximation the retardation leads to additional broadening of transitions participating in the *d-d* interaction, which is related to the van-der Waals interaction between atoms. We estimated that the broadening due to the van-der Waals interaction is two to three orders of magnitude weaker that the spontaneous emission broadening of any Rydberg state considered here, therefore it can be neglected. Though the calculations carried out in this section are only approximate, because we did not take into account the fine structure of Rydberg states, the states, energies, and matrix elements found above should provide a good starting point for evaluating the experimental parameters.

V. TWO-ATOM OPERATIONS

This section presents the analysis of the two-atom gate operations. First we derive a general three-level model for the gate operation in a time-dependent coherent field (Sec. V A). The complete analysis of that model will be carried out elsewhere, here we will be focused on two practically interesting cases where the calculations can be done using two-level approximations. These two cases correspond to exciting either the one-atom resonance (Sec. V B) or the two-atom resonance (Sec. V C): the frequency shift between these two resonances is just the effect of the *d-d* interaction. As we will show, in the first case the gate operation is much less sensitive to small fluctuations in the interatomic distance than in the second case; this will be discussed in Sec. V C.

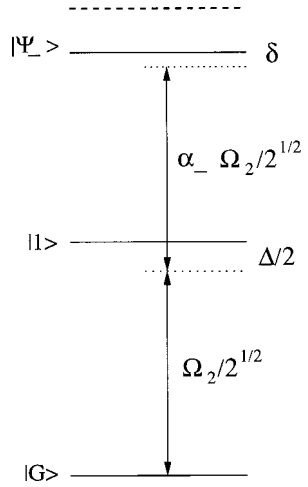

FIG. 5. Level scheme for two atoms with the resonant interaction. The bold dashed line is the position of the two atomic excited state without the dipole-dipole interaction.

We consider now two atoms $k = 1,2$ (prepared initially in $|g\rangle$ states) that strongly interact during the two-photon transition $|g\rangle_k \to |5p_{1/2}\rangle_k \to |42s\rangle_k$ and back, when atoms pass through Rydberg states. When both atoms are excited to their Rydberg states we have to consider the states of the two-atom system determined in the preceding section. There are three two-atom states that participate in the interaction with the field: the ground state $|G\rangle = |g\rangle_1|g\rangle_2$, the symmetric state

$$|1\rangle = \frac{1}{\sqrt{2}}(|42s\rangle_1|g\rangle_2 + |g\rangle_1|42s\rangle_2) \tag{16}$$

with only one atom excited, and the two-atom Rydberg state $|\psi_-\rangle$ determined by Eq. (14). The energy levels of $|G\rangle$, $|1\rangle$, and $|\psi_-\rangle$ states are shown in Fig. 5. The antisymmetric state with one excited atom [similar to Eq. (16), but with sign $-$] and the nonresonant two-atom Rydberg states do not participate in the transition. The two-photon Rabi frequency Ω_2 is given by Eq. (4).

A. General equations

The effective Hamiltonian for the three-level system shown in Fig. 5 is

$$H = H_0 - \frac{\hbar}{2}\sum_{k=1,2}[\Omega_2^{(k)}(t)e^{i(\omega t+\theta_0)} + \text{c.c.}], \tag{17}$$

where $\Omega_2^{(k)}(t)$ is a real function of time, θ_0 is a constant, and $\omega = \omega_{trap} + \omega_{blue}$. The (diagonal) matrix elements of H_0 are $\langle G|H_0|G\rangle = 0$, $\langle 1|H_0|1\rangle = \hbar\tilde{\omega}(t)$, and $\langle\psi_-|H_0|\psi_-\rangle = \hbar[2\tilde{\omega}(t) - \Delta_{d\text{-}d}]$. It is shown in Appendix A that

$$\tilde{\omega}(t) = \omega_0 + \frac{\Omega_{trap}^2}{4\Delta_1} - \frac{\Omega_{blue}^2(t)}{4\Delta_1},$$

where ω_0 is the frequency of the two-photon transition for a single atom in free space, and the two other terms are due to dynamical Stark shifts of the two-photon transitions. The coupling matrix elements are

$$\langle G|\Omega_2^{(k)}|1\rangle=\langle 1|\Omega_2^{(k)}|G\rangle=\Omega_2/\sqrt{2},$$

$$\langle 1|\Omega_2^{(k)}|\psi_-\rangle=\langle \psi_-|\Omega_2^{(k)}|1\rangle=\Omega_2\alpha_-/\sqrt{2}. \tag{18}$$

We suppose that the typical evolution rate of the system is greater that the spontaneous decay rate of the Rydberg states, and we neglect spontaneous emission. We write the wave function of two atoms

$$|\psi_2\rangle=A|G\rangle+Ce^{-i(\omega t+\theta_0)}|1\rangle+Be^{-2i(\omega t+\theta_0)}|\psi_-\rangle, \tag{19}$$

and insert it into the equation $i\hbar d|\psi_2\rangle/dt=H|\psi_2\rangle$, neglecting the fast-oscillating terms. After this we obtain the set of equations for coefficients A, C, and B,

$$i\dot{A}=-\frac{\Omega_2(t)}{\sqrt{2}}C,$$

$$i\dot{C}=\left[\frac{\Delta}{2}-\frac{\Omega_{st}(t)}{2}\right]C-\frac{\Omega_2(t)}{\sqrt{2}}(\alpha_-B+A), \tag{20}$$

$$i\dot{B}=-[\delta+\Omega_{st}(t)]B-\alpha_-\frac{\Omega_2(t)}{\sqrt{2}}C,$$

where

$$\delta=\Delta_{d\text{-}d}-\Delta,\quad \Delta/2=\omega_0-\omega+\Omega/2,$$

$$\Omega=\Omega_{trap}^2/(2\Delta_1),\quad \Omega_{st}(t)=\Omega_{blue}^2(t)/(2\Delta_1).$$

We note that the value of Δ is fixed and determined by ω_{trap} and ω_{blue}, while the detuning δ varies due to fluctuations in the interatomic distance. In general, Eqs. (20) can be solved only numerically. However one can find analytical solutions at least in two special cases, where Eqs. (20) can be reduced to equations for an effective two-level atom.

In the first case we suppose $\Delta\ll\delta\approx\Delta_{d\text{-}d}$ and also $\Omega_{st}(t),\Omega_2(t)\ll\Delta_{d\text{-}d}$. Taking into account that for our values of parameters $\Omega_{trap}\gg\Omega_{blue}(t)$, these requirements can be reduced to the condition

$$\Omega_2(t)/\Delta_{d\text{-}d}\equiv K_1\ll 1. \tag{21}$$

Supposing that the inequality (21) is fulfilled we can adiabatically eliminate B from Eqs. (20), leading to equations for an effective two-level atom

$$i\dot{A}=-\frac{\Omega_2(t)}{\sqrt{2}}C,$$

$$i\dot{C}=\left[\frac{\Delta}{2}-\frac{\tilde{\Omega}_{st}(t)}{2}\right]C-\frac{\Omega_2(t)}{\sqrt{2}}A, \tag{22}$$

where

$$\tilde{\Omega}_{st}(t)=\Omega_{st}(t)\left[1-\alpha_-^2\frac{\Omega}{\delta}\right],\quad \delta\approx\Delta_{d\text{-}d}\gg\Delta. \tag{23}$$

Equations (22) describe a two-photon transition to the two-atom state with only one excited atom. With the condition (21) the state with two excited atoms is never populated, however the presence of this state leads to a Stark shift. Here the dipole-dipole interaction ''removes'' the state with two excited atoms from the interaction with the laser fields die to a dipole blockade [21].

In the second case we suppose $\Delta\approx\Delta_{d\text{-}d}\gg\delta$, assuming again that inequality (21) is verified. By eliminating adiabatically C from Eqs. (20) we obtain

$$i\dot{A}=-\frac{\Omega_4(t)}{2}(A+\alpha_-B),$$

$$i\dot{B}=-[\delta+\Omega_{st}(t)]B-\alpha_-\frac{\Omega_4(t)}{2}(A+\alpha_-B), \tag{24}$$

where Ω_4 is determined by Eq. (5). Equations (24) describe the four-photon transition from the lowest state to the highest state of the two-atom system and Ω_4 is the four-photon Rabi frequency. The state with one excited atom is out of resonance, it has a negligible small population, however it leads to a dynamical Stark shift of the transition.

The solutions of Eqs. (22) and (24) will be found and analyzed in the following sections.

B. "Square pulse" excitation and gate operations with only one excited atom

1. Gate operation

Let us consider the case described by Eqs. (22). The detuning $\delta\sim\Delta_{d\text{-}d}$, which depends on the distance between atoms, appears only in the dynamical Stark shift in Eq. (23). For reliable gate operation it is important to reduce the influence of fluctuations of δ due to possible variations of the distance between the atoms. This takes place when

$$\frac{\alpha_-^2\Omega}{\Delta_{d\text{-}d}}\equiv\frac{\alpha_-^2\Omega_{trap}^2}{2\Delta_1\Delta_{d\text{-}d}}\equiv K_2\ll 1, \tag{25}$$

i.e., when the d-d interaction is large enough, so that $\tilde{\Omega}_{st}(t)\approx\Omega_{st}(t)$.

A simple analytical solution of Eqs. (22) can be found by assuming that the blue field is a square pulse, that is,

$$\Omega_{blue}(t)=\text{const},\quad 0<t<\tau,$$

$$\Omega_{blue}(t)=0,\quad t\leqslant 0,\quad t\geqslant\tau. \tag{26}$$

The approximation (26) is correct when the time of the increase (decrease) of $\Omega_{blue}(t)$ from 0 to its maximum (and back) is much smaller than the pulse duration τ, which is about 10 μs as we will see. This is easily achieved in practice using fast modulators. Assuming that $\Omega_2(t)=\Omega_2$ and $\Omega_{st}(t)=\Omega_{st}$ are constant in Eqs. (22), we find

$$A(t)=e^{-i\lambda_0 t}\left[\cos(\lambda_1 t)+i\frac{\lambda_0}{\lambda_1}\sin(\lambda_1 t)\right], \tag{27}$$

$$C(t)=\frac{i\Omega_2}{\sqrt{2}\lambda_1}e^{-i\lambda_0 t}\sin(\lambda_1 t), \tag{28}$$

where

$$\lambda_0=\frac{\Delta-\Omega_{st}}{4},\quad \lambda_1=\frac{1}{2}\sqrt{\frac{(\Delta-\Omega_{st})^2}{4}+2\Omega_2^2}, \tag{29}$$

with the initial conditions $A(0)=1$ and $C(0)=0$. One can see from Eq. (28) that the square pulse excites the atoms and returns the population back to the ground state if $\tau=\tau_m$, with $\tau_m=\pi m/\lambda_1\approx\sqrt{2}\pi m/\Omega_2$, and $m=1,2,\ldots$. Using Eq. (27) one obtains $A(\tau_m)=(-1)^m e^{-i\lambda_0\tau_m}$, so that the effect of the square pulse of duration τ_m is

$$|g\rangle_1|g\rangle_2\rightarrow e^{-i\varphi_m}|g\rangle_1|g\rangle_2,\quad \varphi_m=\lambda_0\tau_m+\pi m. \tag{30}$$

It is easy to check that the pulse does not interact with an atom in the $|e\rangle$ state, provided that $m\Omega_2\ll\omega_F$, so that the state $|e\rangle_1|e\rangle_2$ is unchanged. In order to complete transformation (1), the square pulse of duration τ_m has to provide

$$|g\rangle\rightarrow e^{-i\tilde{\varphi}}|g\rangle \tag{31}$$

for the single-atom case, with $2\tilde{\varphi}\neq\varphi_m$. For describing that case we note that Eqs. (22) with $\tilde{\Omega}_{st}(t)\approx\Omega_{st}(t)$ are almost identical to the single-atom Eqs. (A3) from Appendix A, except for the replacement of the factor $\Omega_2(t)/2$ in Eqs. (A3) by $\Omega_2(t)/\sqrt{2}$ in Eqs. (22). This is due to the cooperative character of the two-atom excitation, which disappears for one atom only. Therefore the transformations (30) and (31) are generally not compatible: if there is initially only one atom in the $|g\rangle$ state, it may be left in the excited state after the laser excitation. In order to find for which parameter values the transformations (30) and (31) are both possible, we consider the results (27)–(29), with appropriate changes in the Rabi frequency. The duration of the square pulse for completing a single-atom excitation is thus

$$\tilde{\tau}_n=\pi n/\tilde{\lambda}_1,\quad n=1,2\ldots, \tag{32}$$

where

$$\tilde{\lambda}_1=\frac{1}{2}\sqrt{\frac{(\Delta-\Omega_{st})^2}{4}+\Omega_2^2} \tag{33}$$

and the probability amplitude for the low atomic state after that pulse is $A_1(\tilde{\tau}_n)=(-1)^n e^{-i\lambda_0\tilde{\tau}_n}$.

In order to obtain the transformations (30), (31) for a given square pulse of duration τ, one needs $\tau=\tau_m=\tilde{\tau}_n$, which is obtained when

$$\Delta=\Omega_{st}\pm 2\Omega_2\sqrt{\frac{2n^2-m^2}{m^2-n^2}}. \tag{34}$$

Under this condition

$$\tau_m=\frac{2\pi}{\Omega_2}\sqrt{m^2-n^2},\quad \varphi_m=\pi(m\pm\sqrt{2n^2-m^2}),$$
$$\tilde{\varphi}=\tilde{\varphi}_n=\pi(n\pm\sqrt{2n^2-m^2}), \tag{35}$$

so that the transformation of the two-atom states is

$$\begin{aligned}
&|e\rangle|e\rangle\rightarrow|e\rangle|e\rangle,\\
&|e\rangle|g\rangle\rightarrow e^{-i\tilde{\varphi}_n}|e\rangle|g\rangle,\\
&|g\rangle|e\rangle\rightarrow e^{-i\tilde{\varphi}_n}|g\rangle|e\rangle,\\
&|g\rangle|g\rangle\rightarrow e^{-i\varphi_m}|g\rangle|g\rangle.
\end{aligned} \tag{36}$$

Proceeding the single-atom operation (3) with $\varphi_0=\tilde{\varphi}_n$ as is described in Sec. III we achieve the transformation (1) with

$$\varphi=2\tilde{\varphi}_n-\varphi_m=\pi(-m\pm\sqrt{2n^2-m^2}), \tag{37}$$

where the sign must be the same as in Eq. (34). One can see that Eq. (34) has real solution for $m>n$ and $m\geqslant 4$. Taking $m=4$, $n=3$ and choosing "$-$" in Eq. (34) we obtain

$$\Delta=\Omega_{st}-2\Omega_2\sqrt{\frac{2}{7}},\quad \tau_m=\frac{2\pi\sqrt{7}}{\Omega_2},$$
$$\tilde{\varphi}_n=\pi(1-\sqrt{2}),\quad \varphi=-\pi\sqrt{2}. \tag{38}$$

2. Optimization of the interatomic distance

For a convenient operation of the gate, we seek a switching time as short as possible, which is anyway much shorter than the spontaneous emission time of the Rydberg states. Faster gate operation is obtained by increasing the two-photon Rabi frequency, but this increase has to be consistent with all other requirements (the size of the *d-d* interaction, nonresonant approximations, etc). As a result, we will show now that faster gate operation requires both increasing the laser powers and decreasing the interatomic distance. We choose $K_2=0.1$, which satisfies inequality (25) at the maximum value of Ω_{trap}, which may be necessary for the reliable dipole trap operation. Preserving condition (25) with fixed K_2 for various distances r between atoms we must change Ω_{trap} according to the relation

$$\Omega_{trap}(r)=\frac{\sqrt{2K_2\Delta_1\Delta_{d\text{-}d}(r)}}{\alpha_-(r)}, \tag{39}$$

where $\Delta_{d\text{-}d}(r)$ and $\alpha_-(r)$ can be found with the help of Eqs. (15). In a similar way one can obtain the value of Ω_{blue} for various r, inserting $\Omega_{trap}(r)$ from Eq. (39) into Eq. (21),

$$\Omega_{blue}(r)=\frac{K_1\alpha_-(r)}{\sqrt{K_2}}\sqrt{2\Delta_1\Delta_{d\text{-}d}(r)}. \tag{40}$$

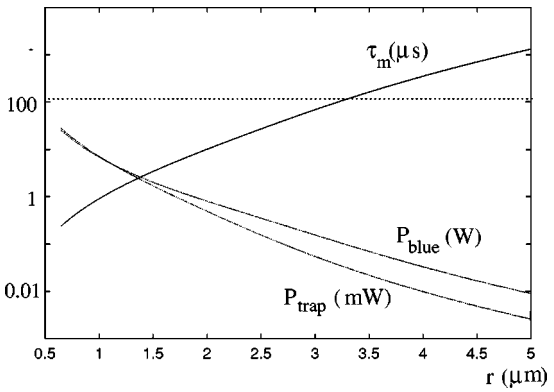

FIG. 6. Power of the blue laser and the dipole trap laser, and gate operation time as a function of the interatomic distance, when the gate interacts with the square pulse. The horizontal dotted line marks the spontaneous emission time of the Rydberg states.

From the relation (21) and the result (38) for the pulse duration τ_m we find the variation of the gate operation time with the interatomic distance

$$\tau_m(r)=\frac{2\pi\sqrt{7}}{K_1\Delta_{d\text{-}d}(r)}. \tag{41}$$

Equations (39) and (40) and the experimental requirement $\Omega_{blue}\ll\Omega_{trap}$ are consistent when $K_1/K_2\ll 1$. Then from Eqs. (39) and (40) one can calculate the laser powers and the gate operating time as a function of the interatomic distance. This is shown on Fig. 6 for $K_2=0.1$, $K_1=0.001$ and the values of other parameters presented before. One can see that the optimal distance between atoms is about 1.5–2 μm, which corresponds to the power of trap and blue fields, $\sim$0.1–1 mW and $\sim$0.1–1 W, respectively, with the gate operation time $\tau_m\sim$10–1 μs. The horizontal dotted line in Fig. 6 shows the spontaneous emission time of the Rydberg states. It can also be checked that by decreasing r and increasing Ω_{blue}, Ω_{trap} does not lead to the excitation of atoms from the $|e\rangle$ ground state, as long as the interatomic distance r is larger than 0.65 μm.

An attractive feature of this ''square pulse excitation'' regime is that it is not very sensitive to the fluctuations in the interatomic distance [as far as condition (25) is true]. However one can obtain only certain values of the phase φ in this regime, as one can see from Eq. (37). If arbitrary values of φ are necessary, one may change the pulse profile providing, at the same time, the compatibility between the two-atom and the one-atom operations as above, or utilize the self-transparency regime described in the following section.

C. Gate operation with simultaneous excitation of two atoms

1. Self-transparency regime

Now let us consider the case of Eqs. (24), where we set $\Delta=\Delta_{d\text{-}d}$ for the average interatomic distance. We can look for a solution of Eq. (24) while a 2π-pulse $\Omega_{blue}(t)$ excites the atoms and returns all the population back to the low state for any value of δ. Let us introduce the pulse area

$$\theta(t)=\frac{1}{2}\int_{-\infty}^{t}\Omega_4(t')dt'.$$

Calculations carried out in Appendix D lead to the solution of Eqs. (24) for a pulse of duration τ,

$$A(t)=\frac{\cos\theta(t)-i\tau\delta}{1-i\tau\delta}e^{i\theta(t)},$$

$$B(t)=\frac{i\sin\theta(t)}{\alpha_-(1-i\tau\delta)}e^{i\theta(t)}, \tag{42}$$

with the initial conditions $A(t\to-\infty)=1$ and $C(t\to-\infty)=0$ and with $\theta(t)$ satisfying Eq. (D9) of Appendix D. The 2π pulse $\int_{-\infty}^{\infty}\Omega_4(t')dt'=2\pi$ returns all the population back to the low level and leads to

$$A(t\to\infty)=\frac{1+i\tau\delta}{1-i\tau\delta}\equiv e^{i\varphi'},\quad \varphi'=i\ln\frac{1-i\tau\delta}{1+i\tau\delta}. \tag{43}$$

Therefore the 2π pulse provides the two-atom transformations

$$\begin{aligned}
&|e\rangle|e\rangle\to|e\rangle|e\rangle,\\
&|e\rangle|g\rangle\to i|e\rangle|g\rangle,\\
&|g\rangle|e\rangle\to i|g\rangle|e\rangle,\\
&|g\rangle|g\rangle\to e^{i\varphi'}|g\rangle|g\rangle
\end{aligned} \tag{44}$$

and the one-atom transformation $|g\rangle\to i|g\rangle$. We note that, different from the previous case, now both atoms are always left in the ground state, so that no special care about the compatibility between the one-atom and the two-atom operations is necessary, which is one of the advantages of the ''self-transparency'' regime of excitation.

In order to correct for the i phase shift one may use the one-atom transformation (5) with $\Delta=-\Delta_{d\text{-}d}$ after the transformation (44). Indeed, for $\Delta=-\Delta_{d\text{-}d}$ the four-photon excitation of two atoms is out of resonance and can be neglected, while the change of the phase of an atom in the $|e\rangle$ state is still negligible small, because $\omega_F\gg\Delta_{d\text{-}d}$. Therefore for $\Delta=-\Delta_{d\text{-}d}$ the atom-field interaction leads to

$$\begin{aligned}
&|e\rangle|e\rangle\to|e\rangle|e\rangle,\\
&|e\rangle|g\rangle\to -i|e\rangle|g\rangle,\\
&|g\rangle|e\rangle\to -i|g\rangle|e\rangle,\\
&|g\rangle|g\rangle\to -|g\rangle|g\rangle.
\end{aligned} \tag{45}$$

It is thus clear that applying the transformations (44) and (45) one after the other leads to the expected transformation (1) with $\varphi=\pi+\varphi'$.

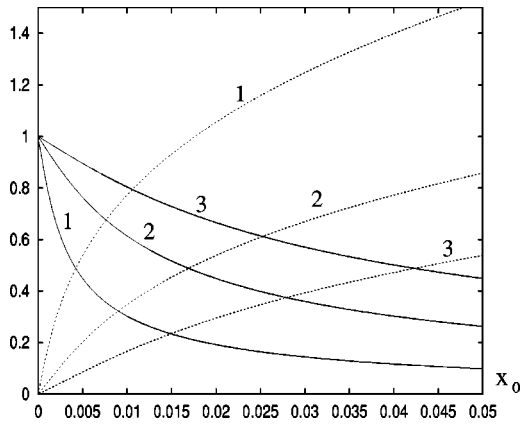

FIG. 7. Average $(1/\pi)\langle\varphi\rangle$ (solid curves) and relative dispersion of the phase fluctuations (dotted curves) for $\Delta_{d\text{-}d}\tau=100$ (curves 1), 25 (curves 2) and 10 (curves 3) as functions of $x_0=\sqrt{\langle\delta r^2\rangle}/r$.

2. Effect of small fluctuations in the interatomic distance

The detuning δ in Eq. (24) may fluctuate due to fluctuations in the interatomic distance. The best situation is, therefore, when any term that depends on δ can be neglected. Such terms are present in Eq. (43) for the phase φ' and in Eq. (D9) of Appendix D, which determines the pulse area $\theta(t)$. They can be neglected in both Eqs. (43) and (D9) when

$$\left[\frac{2\Delta_{d\text{-}d}\Delta_1}{\Omega_{trap}^2}+\alpha_-^2-1\right]\ll\tau\delta\ll 1. \tag{46}$$

In our case $\alpha_-^2\approx 1$, so that the inequality (46) needs $2\Delta_{d\text{-}d}\Delta_1/\Omega_{trap}^2\ll 1$, which is opposite to the condition (25) found for the case with only one excited atom. With the condition (46) $\varphi'=0$, $A(t\to\infty)=1$, and $\theta(t)=2\arctan[\exp(t-t_0/\tau)]$, which corresponds to the well-known expression for 2π pulse,

$$\Omega_4(t)=\frac{2}{\tau}\mathrm{sech}\left(\frac{t-t_0}{\tau}\right). \tag{47}$$

Using the value $P_{trap}=2.5$ mW, which corresponds to $\Omega_{trap}=2.31\times 10^{11}\ \mathrm{s}^{-1}$, we obtain $2\Delta_{d\text{-}d}\Delta_1/\Omega_{trap}^2<0.01$ for the interatomic distance $r\geqslant 4\ \mu$m. The condition $\tau\delta\ll 1$ can be satisfied, in principle, either for small δ or for small τ. However the only case of small δ is in accordance with the assumption $\Delta\approx\Delta_{d\text{-}d}\gg\Omega_2$ made at the derivation of Eqs. (24) from Eq. (20).

Assuming a Gaussian distribution function $f(x)=(x_0\sqrt{\pi})^{-1}\exp(-x^2/x_0^2)$, where $x_0=\sqrt{\langle\delta r^2\rangle}/r$ for the relative distance fluctuations $x=\delta r/r$, we calculated the average phase $\langle\varphi\rangle=\langle\varphi'\rangle+\pi$ and the dispersion $\sqrt{\langle\varphi^2\rangle-\langle\varphi\rangle^2}/\langle\varphi\rangle$. These quantities are shown in Fig. 7 as functions of x_0 for $\Delta_{d\text{-}d}\tau=100$, 25, 10, which corresponds, respectively, to $P_{blue}=0.8$, 3.2, and 8 W. These curves show clearly that this scheme is very sensitive to distance fluctuations.

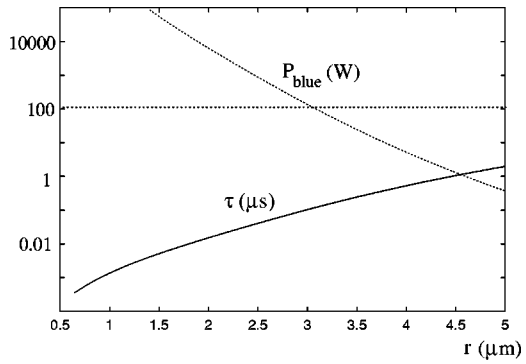

FIG. 8. Power of the blue laser and gate operation time as a function of the interatomic distance in the self-transparency regime of the gate operation when $P_{trap}=2.5$ mW. The horizontal dotted line marks the spontaneous emission time of Rydberg states.

3. Optimization of the interatomic distance

As in Sec. V B, the parameters of the gate operation can be optimized for various interatomic distances, using the conditions (21) and (46) and looking for a fast gate operation. The fast gate operation needs the highest possible value for the effective four-photon Rabi frequency Ω_4, which can be achieved with a few milliwatts of power of the trap field under our experimental conditions. When the inequality (46) is satisfied, the operation time of the trap can be estimated from Eq. (47),

$$\tau=2/\Omega_4=\frac{4\Delta\Delta_1^2}{[\Omega_{trap}\Omega_{blue}(t)]^2}, \tag{48}$$

where Eqs. (5) and (4) for Ω_4 have been used. In order to preserve condition (21) with a small K_1 for various interatomic distances, we have to choose $\Omega_{blue}(r)$ according to the relation

$$\Omega_{blue}(r)=2K_1\frac{\Delta_{d\text{-}d}(r)\Delta_1}{\Omega_{trap}}. \tag{49}$$

Inserting $\Omega_{blue}(r)$ into Eq. (48) and taking into account that $\Delta=\Delta_{d\text{-}d}$ we obtain τ as a function of the interatomic distance r,

$$\tau(r)=\frac{1}{K_1^2\Delta_{d\text{-}d}(r)}. \tag{50}$$

Figure 8 shows the curves $\Omega_{blue}(r)$ and $\tau(r)$ obtained with the help of Eqs. (49) and (50) for $K_1=0.2\ll 1$. It follows from Eq. (50) that $\tau(r)\Delta_{d\text{-}d}(r)=K_1^{-2}=25$, which corresponds to curves 2 in Fig. 7. These curves point out that the gate reliably operates only for very small relative interatomic distance fluctuations $x_0<0.01$. It is more easy to provide smaller relative distance fluctuations for larger distances. Therefore, the best distance between atoms is now in the extreme left of Fig. 8, which is about 4–5 μm, which corresponds, respectively, to $\tau\sim 0.53$–2 μs for $P_{blue}\sim 5$–0.37 W. For larger interatomic distances the gate op-

eration time τ is approaching the spontaneous emission time of Rydberg states, which is marked by the horizontal dashed line in Fig. 8.

VI. SUMMARY AND DISCUSSION

We studied two regimes of operation of a conditional quantum phase gate realized on two neutral atoms in two separate optical dipole traps at a distance $r \sim 1-5$ μm. The atoms are coupled with each other through the dipole-dipole (d-d) interaction induced by a two-photon transition of the atoms to Rydberg states with $n \approx 40$. The two-photon transition is carried out by two fields, one of them is the constant dipole trap field with $\lambda_{trap} \approx 802.3$ nm, with a beam cross section $S_{trap} \approx 10^{-8}$ cm^2 and a power of a few milliwatts. Another is a time-dependent field with $\lambda_{blue} \approx 472.7$ nm, beam cross section $S_{blue} \approx 10^{-6}$ cm^2, and power $P_{blue} \sim 0.1-10$ W. It was found that the typical gate operation time is $\sim 1-10$ μs. We note that in Ref. [5] the authors supposed a much smaller interatomic distance, $r \sim 0.3$ μm, and could reach a much faster operation time of the gate ~ 10 ns. But accurate control and addressing of a single atom at such a small distance is clearly more difficult in the experimental conditions of [7]. An advantage of a very fast operation is that the atoms do not move during the gate operation. Here this condition is only approximately satisfied, but the analysis of such motional effects is beyond the scope of the present paper.

In the first regime, described in Sec. V B, only one of the two atoms can be excited, and the state with two excited atoms is shifted from resonance due to d-d interaction. In this regime one can neglect the influence of the fluctuations in the interatomic distance, provided that the d-d interaction is large enough, which is the case for our parameter values. In Sec. V B we considered an example of the excitation of atoms by a ''square'' pulse, which allowed us to simplify the analysis of the gate operation and to get analytical results. However exciting the atoms with a square pulse permits only certain values for the conditional phase φ, which are irrational fractions of π [see Eq. (37)]. This is not appropriate for a full quantum controlled-NOT gate operation. If an arbitrary value of φ is necessary, the scheme of Sec. V B has to be generalized to more complicated pulses profiles. The pulse profile and the energy corresponding to an arbitrary φ, and still returning all the atomic population to the ground state, can be found by numerical analysis of Eqs. (22), which will be carried out elsewhere.

In the second ''self-transparency'' gate operation regime described in Sec. V C the two atoms can be excited simultaneously only, and the state with a single excited atom is out of resonance. In this regime one can obtain $\varphi = \pi$ and realize a full quantum controlled-NOT gate operation. This can be achieved by driving atom 2 with a $\pi/2$ Raman pulse to obtain $|g\rangle_2 \rightarrow (1/\sqrt{2})(|e\rangle_2 + |g\rangle_2)$, $|e\rangle_2 \rightarrow (1/\sqrt{2})(|e\rangle_2 - |g\rangle_2)$, then applying the transformation (1) with $\varphi = \pi$, and finally driving again atom 2 with another $\pi/2$ pulse. These three transformations are equivalent to the controlled-NOT map, when atom 2 changes (or preserves) its state at the condition that atom 1 is in $|g\rangle$ (or $|e\rangle$) state. In the absence of fluctuations when the detuning δ is fixed, one can achieve an arbitrary value for φ in this second regime—see Eq. (43). The advantage of the ''self-transparency'' regime is, therefore, that the same pulse profile provides an arbitrary desirable conditional phase leaving both atoms in the ground state after the excitation. However the estimations of Sec. V C show that the gate reliably operates in this regime only when the fluctuations in the interatomic distance are very small.

Thus each regime considered here has its advantages and disadvantages. We note that there are more free parameters in the general case described by Eqs. (20), when all three relevant levels of the two-atom system (see Fig. 5) are involved in the interaction with the field. Therefore, it may be possible to find a better compromise for both eliminating the effect of the distance fluctuations and obtaining an arbitrary conditional phase φ (one may also use a sequence of pulses as proposed in [10]). A full optimization requires a numerical analysis of the set of equations (20), which will be carried out elsewhere.

The general results of analysis of the d-d interaction and the two gate operation regimes carried out in Secs. IV and V can be applied also to other entangled quantum two-level systems used as qubits as, for example, quantum dots.

As a final conclusion, the present study makes clear that both the value and the fluctuations in the interatomic distance are crucial parameters when it comes to using free-space d-d interaction for a quantum gate. This stringent requirement might be somehow relaxed by using cavity-assisted collisions [22].

ACKNOWLEDGMENTS

This work was supported by the European IST/FET program ''QUBITS'' and by the European IHP network ''QUEST.'' I.E.P. is also grateful to the Russian Foundation for Basic Research, Grant No. 01-02-17330, for support.

APPENDIX A

Let us analyze the two-photon transition $|5s\rangle \rightarrow |5p_{1/2}\rangle \rightarrow |42s\rangle$. We denote the energy levels 1,2,3 as shown in Fig. 3. The Hamiltonian of the three-level atom is

$$H = H_0 - \hat{\mu}\mathcal{E}(t), \tag{A1}$$

where H_0 is the Hamiltonian of an atom without the interaction with the field, $\langle 1|H_0|1\rangle = 0$, $\langle 2|H_0|2\rangle = \hbar\omega_{12}$, $\langle 3|H_0|3\rangle = \hbar\omega_0$, where $\omega_0 = \omega_{12} + \omega_{23}$, ω_{12} and ω_{23} are transition frequencies, $\hat{\mu}$ is the dipole momentum operator, $\langle 1|\hat{\mu}|2\rangle = \mu_{12}e^{i\theta_{12}}$, $\langle 2|\hat{\mu}|3\rangle = \mu_{23}e^{i\theta_{23}}$, μ_{12}, μ_{23} are real,

$$\mathcal{E}(t) = \mathcal{E}_{trap}\cos(\omega_{trap}t + \varphi_{trap}) + \mathcal{E}_{blue}(t)\cos(\omega_{blue}t + \varphi_{blue}),$$

$\omega_{trap} \approx \omega_{12}$, $\omega_{blue} \approx \omega_{23}$. Taking the wave function

$$\psi = A_1'\psi_1 + A_2 \exp[-i(\omega_{trap}t + \varphi_{trap} + \theta_{12})] + A_3' \exp[-i(\omega_{trap}t + \omega_{blue}t + \varphi_{trap} + \varphi_{blue} + \theta_{12} + \theta_{23})],$$

solving the equation $i\hbar\dot{\psi} = H\psi$, and neglecting the fast-oscillating terms we obtain

$$\dot{A}_1' = i\frac{\Omega_{trap}}{2}A_2,$$

$$\dot{A}_2 = -i\Delta_1 A_2 + i\frac{\Omega_{trap}}{2}A_1' + i\frac{\Omega_{blue}(t)}{2}A_3', \tag{A2}$$

$$\dot{A}_3' = -i\frac{\Delta'}{2}A_3' + i\frac{\Omega_{blue}(t)}{2}A_2,$$

where $\Delta_1 = \omega_{12} - \omega_{trap}$, $\Delta'/2 = \omega_0 - \omega_{trap} - \omega_{blue}$, $\Omega_{trap} = \mu_{12}\mathcal{E}_{trap}/\hbar$, $\Omega_{blue}(t) = \mu_{23}\mathcal{E}_{blue}(t)/\hbar$. Supposing $\Delta_1 \gg \Omega_{trap}, \Omega_{blue}$ we eliminate adiabatically A_2 from Eqs. (A2), which leads to

$$\dot{A}_1' = i\frac{\Omega}{2}A_1' + i\frac{\Omega_2(t)}{2}A_3',$$

$$\dot{A}_3' = -i\left[\frac{\Delta'}{2} - \frac{\Omega_{st}(t)}{2}\right]A_3' + i\frac{\Omega_2(t)}{2}A_1,$$

where $\Omega_2(t) = \Omega_{trap}\Omega_{blue}(t)/(2\Delta_1)$ is the two-photon Rabi frequency, $\Omega = \Omega_{trap}^2/(2\Delta_1)$, $\Omega_{st}(t) = \Omega_{blue}^2(t)/(2\Delta_1)$. Because $\Omega = \text{const}$ one can take into account a constant Stark shift of the states $|1\rangle$, $|3\rangle$ in the trap field by setting

$$A_k' = A_k e^{i\Omega t/2}, \quad k = 1,3$$

so that

$$\dot{A}_1 = i\frac{\Omega_2(t)}{2}A_3,$$

$$\dot{A}_3 = -i\left[\frac{\Delta}{2} - \frac{\Omega_{st}(t)}{2}\right]A_3 + i\frac{\Omega_2(t)}{2}A_1, \tag{A3}$$

where $\Delta/2 = \Delta'/2 + \Omega/2$. Equations (A3) are equivalent to the equations for an effective two-level atom with the time-dependent transition frequency

$$\tilde{\omega}(t) = \omega_0 + (1/2)[\Omega - \Omega_{st}(t)].$$

Such a two-level atom interacts with the effective field with the carrier frequency $\omega = \omega_{trap} + \omega_{blue}$ and the effective Rabi frequency $\Omega_2(t)$. When $\Delta \gg \Omega_{st}(t), \Omega_2(t)$ one can adiabatically eliminate A_3 from Eqs. (A3), find $A_3 \approx [\Omega_2(t)/\Delta]A_1$ and obtain the result (5).

APPENDIX B

Here we present the calculations of the oscillator strengths for transitions to the Rydberg states of ^{87}Rb atom. Rabi frequency for $\nu - \nu'$, $\nu = \{n,l\}$ one-photon transition is

$$\Omega_{\nu\nu'} = \frac{|\mu_{\nu\nu'}|}{\hbar}\sqrt{\frac{W_{\nu\nu'}}{\pi S_{\nu\nu'}c_0^3}}, \tag{B1}$$

where $\mu_{\nu\nu'}$ is the matrix element of the dipole momentum, $W_{\nu\nu'}$ and $S_{\nu\nu'}$ are the power (in erg) and the cross section (in cm^2) of the laser beam resonant to the transition, respectively; c_0 is the light speed in vacuum. In order to find $\mu_{\nu\nu'}$ we have to calculate the oscillator strength

$$f_{\nu\nu'} = -\frac{2m\omega_{\nu\nu'}|\mu_{\nu\nu'}|^2}{3\hbar e^2}, \tag{B2}$$

where $\omega_{\nu\nu'} = (E_\nu - E_{\nu'})/\hbar$, E_ν is the energy of the state ν, m is the electron mass, e is the electron charge. Formula (B2) can be written in terms of the atomic energy unit $E_{at} = me^4/\hbar^2$ and Bohr radius $a_0 = \hbar^2/(me^2)$ as

$$f_{\nu\nu'} = -\frac{2}{3}\frac{\hbar\omega_{\nu\nu'}}{a_0^3 E_{at}^2}|\mu_{\nu\nu'}|^2.$$

Normalizing the distance r from the nuclear to an electron to a_0, taking $\omega_{\nu\nu'}$ in cm^{-1} and introducing the Rydberg constant $R = 0.5E_{at} = 109\,737.257$ cm^{-1}, proceeding the integration over the angular variables of wave functions and summing over all components of a multiplet (see [23], p. 221), one can find

$$f_{\nu\nu'} = -\frac{\omega_{\nu\nu'}}{3R}\frac{l_{max}}{2l+1}(\mathcal{R}_{\nu\nu'})^2, \tag{B3}$$

where $l_{max} = \max\{l,l'\}$,

$$\mathcal{R}_{\nu\nu'} = \int_0^\infty P_\nu(r)P_{\nu'}(r)r\,dr. \tag{B4}$$

$P_\nu(r) = r\mathcal{R}_\nu(r)$, $\mathcal{R}_\nu(r)$ is the radial wave function of the state ν. For $np_{1/2} \to n's$ and $np_{3/2} \to n's$ transitions one has to take the oscillator strengths $f_{\nu\nu'}/3$ and $2f_{\nu\nu'}/3$, respectively.

The radial wave function can be calculated in the approximation of Bates and Damgaard [24],

$$P_\nu(r) = \left(\frac{2r}{n_\nu^*}\right)^{n_\nu^*}\exp\left(\frac{r}{n_\nu^*}\right)\sum_{k=0}^{k_{max}}\frac{a_k}{r^k}, \tag{B5}$$

where n_ν^* is an effective quantum number,

$$n_\nu^* = \sqrt{\frac{R}{E_i - E_\nu}}, \tag{B6}$$

$E_i = 33\,691.02$ cm^{-1} is the energy of ionization of ^{87}Rb, the energy E_ν of the state ν is determined from the experiment, k_{max} is the maximum integer smaller than $n_\nu^* + 1$, and the coefficients a_k can be found from the recurrent relations

TABLE I. Oscillator strengths for $5s \rightarrow np$ transitions.

np	Method [24]	From Ref. [25]
$5p$	1.028	1.033
$6p$	0.0277	0.0266
$7p$	6.69×10^{-3}	6.18×10^{-3}
$8p$	2.72×10^{-3}	2.78×10^{-3}
$9p$	1.36×10^{-3}	1.27×10^{-3}
$10p$	7.63×10^{-4}	7.44×10^{-4}
$11p$	4.53×10^{-4}	4.82×10^{-4}
$12p$	2.81×10^{-4}	3.34×10^{-4}

$$a_0=\frac{1}{n_\nu^*}\left[\frac{1}{\Gamma(n_\nu^*+l+1)\Gamma(n_\nu^*-l)}\right]^{1/2},$$

$$a_k=a_{k-1}\frac{n_\nu^*}{2k}[l(l+1)-(n_\nu^*-k)(n_\nu^*-k+1)]. \quad \text{(B7)}$$

Our numerical procedure of calculation of the wave functions (B5) gives results that are satisfactory for the estimations. In Table I one can compare the oscillator strengths for $5s \rightarrow np$ transitions calculated by using the formula (B5) for $P_\nu(r)$ and the oscillator strengths taken from [25]. In order to find oscillator strengths for any transitions $nl \rightarrow n'l'$ one can use different methods depending on the values of principle quantum numbers n and n'.

(1) The method used in [24] allows us to calculate the oscillator strengths for any transition with $n \leqslant 36$ or 37, while the non-negligible numerical error appears for higher n.

(2) For $n>36$ we can find radial wave functions (B5) if $\Delta n^*_{\nu\nu'} \equiv |n_\nu^* - n_{\nu'}^*| \gg 1$ taking only the part of the function $P_{\max(n_\nu^*, n_{\nu'}^*)}(r)$ for $0<r<r_0$, while the other wave function $P_{\nu'}(r)$ is numerically zero ($<10^{-15}$) for $r>r_0$. For example, $P_{6s}(r)=0$ for $r>r_0=200$, so that we can find the oscillator strength for any $6s \rightarrow \nu'$ transition considering $P_{\nu'}(r)$ only in the interval $0<r<200$.

(3) $n>36$ and $\Delta n^*_{\nu\nu'}=1,2 \ll n_\nu^*, n_{\nu'}^*$. In this case one can use the formula (I.177) of [26] (see also [27]),

$$\mathcal{R}_{\nu\nu'} \approx \frac{3}{2}\left(\frac{2n_\nu^* n_{\nu'}^*}{n_\nu^*+n_{\nu'}^*}\right)^2 g(\Delta n^*_{\nu\nu'}), \quad \text{(B8)}$$

where the dimensionless function $g(\Delta n^*_{\nu\nu'})$ is presented in Fig. 15 of [26].

(4) $n>36$ and $2<\Delta n^*_{\nu\nu'} \leqslant 20$. Here one can use the formula (I.179) of [26],

$$\mathcal{R}_{\nu\nu'} \approx 0.4866\left(\frac{n_\nu^* n_{\nu'}^*}{n_\nu^*+n_{\nu'}^*}\right)^{5/3}(n_\nu^* n_{\nu'}^*)^{1/3}\left[\frac{1}{(\Delta n^*_{\nu\nu'})^{5/3}} - \frac{0.2177}{(\Delta n^*_{\nu\nu'})^{7/3}}\right]\cos[\pi(\Delta n^*_{\nu\nu'}+0.18)]. \quad \text{(B9)}$$

TABLE II. Oscillator strengths for $34s \rightarrow np$ transitions.

np	(B9)	(B5)	(B8)	$\Delta n^*_{\nu\nu'}$
$33p$	2.69	12.18	12.93	0.49
$31p$	0.10	0.16	0.14	2.49
$29p$	0.027	0.036	0.027	4.49
$28p$	0.016	0.022	0.086	5.49
$26p$	0.0077	0.011	0.044	7.49
$20p$	0.0014	0.0021		13.49
$10p$	1.35×10^{-4}	2.71×10^{-4}		23.49

Oscillator strengths for transitions from the $34s$ state to several np states found with the help of formulas (B9), with the wave functions (B5) and the formula (B8) are presented in Table II.

APPENDIX C

A photoionization of trapped atoms may destroy the gate if it goes faster than the typical time of the excitation of atoms to Rydberg states. The strongest channel for the photoionization is the two-step process, when the atom is excited to the Rydberg state; after that the electron from this state is taken away by strong trap field. We estimate the rate of such process as

$$\frac{1}{\tau_{ion}} \approx \frac{\sigma_{ion} I_{trap}}{\hbar \omega_{trap}} \langle |C|^2 \rangle, \quad \text{(C1)}$$

where σ_{ion} is the cross section of the photoionization of the Rydberg state, $I_{trap}=P_{trap}/S_{trap}$ is the trap field intensity, and $\langle |C|^2 \rangle$ is the average population of the Rydberg state during the excitation of the atom. We estimate the upper limit for σ_{ion} by the formula [28] (see also [23], p. 267) that was derived in the approach [24] used in Appendix B in the calculations of oscillator strengths. For the transition between the eigenstate $\nu=\{n,l\}$ of Rb and the free-electron state with the orbital momentum quantum number l' and the energy ϵR, where R is the Rydberg constant, this formula reads

$$\sigma_{ion} \approx 5.45\times10^{-19}\frac{(n_\nu^*)^3}{[1+\epsilon(n_\nu^*)^2]^3}|G(\nu,\epsilon,l') \times \cos\{\pi[n_\nu^*+\Delta(\epsilon)+\chi(n_\nu^*,l,\epsilon l')]\}|^2, \quad \text{(C2)}$$

where σ_{ion} is in cm^2, an effective quantum number n_ν^* is given by the formula (B6) of Appendix B, $\Delta(\epsilon)$ is the extrapolation of the quantum defect $n-n_\nu^*$ to the free-electron energy region, $G(\nu,\epsilon,l')$ and $\chi(n_\nu^*,l,\epsilon l')$ are parameters whose values are presented in [23]. Extrapolating the data of [23] to the case $n_\nu^* \gg 1$ we can estimate $|G(\nu,\epsilon,l')\cos(\pi[n_\nu^*+\Delta(\epsilon)+\chi(n_\nu^* l,\epsilon l')])|^2 \leqslant 1$ and $\sigma_{ion} \leqslant 7\times10^{-21}$ cm^2 for $\nu=(42,s)$ state of ^{87}Rb. Applying formulas (28), (29), (38) and parameters of the trap field used throughout the paper, we find the typical time of ionization $\tau_{ion} \geqslant 128\ \mu s \gg \tau_m \sim 10\ \mu s$, where τ_m is the time of the interaction of the atom with the square pulse of the field. An

alternative estimation for τ_{ion} can be carried out by the formula (II.32) of [26]. Taking into account the average population of the Rydberg state we rewrite this formula in our notations as

$$\frac{1}{\tau_{ion}}=\frac{64\pi}{3}\frac{a_0^3R^2P_{trap}}{c_0\hbar^3\omega_{trap}^2S_{trap}}\frac{\sin^2(2/\epsilon)}{(n\epsilon)^3}\langle|C|^2\rangle, \quad \text{(C3)}$$

where a_0 is the Bohr radius and c_0 is the speed of light. The estimation by formula (C3) gives $\tau_{ion}\sim 380$ μs, which is a value even higher than that by the formula (C2) because of the phase factor $\sin^2(2/\epsilon)\approx 0.1$ preserved in Eq. (C3). Thus for given parameter values the two-step ionization of the Rydberg state by the trap field is a slow process with respect to the gate operation and it does not destroy the gate.

APPENDIX D

Let us show that while $\theta(t)$ is given by Eq. (D9) we obtain the solution of Eqs. (24) given by Eqs. (42). Let us define two new variables $A_0(t)$ and $B_0(t)$ such that

$$A(t)=\alpha_- A_0(t)e^{i\theta(t)}, \quad B(t)=B_0(t)e^{i\theta(t)}. \quad \text{(D1)}$$

Inserting the expressions (D1) into Eqs. (24) we obtain

$$i\dot{A}_0=-\dot{\theta}(t)B_0,$$

$$i\dot{B}_0=-[\delta+\dot{\theta}(t)(\xi+\alpha_-^2-1)]B_0-\dot{\theta}(t)A_0, \quad \text{(D2)}$$

where we replaced $\Omega_{st}=\xi\Omega_4/2$ with $\xi=2\Delta_{d\text{-}d}\Delta_1/\Omega_{trap}^2$ and set $\Delta=\Delta_{d\text{-}d}$, $\Omega_4/2=\dot{\theta}(t)$. Let us separate $A_0=A_1+iA_2$, $B_0=B_1+iB_2$, and write the equations for the real and imaginary parts of A_0 and B_0,

$$\dot{A}_1=-\dot{\theta}(t)B_2,$$

$$\dot{A}_2=\dot{\theta}(t)B_1, \quad \text{(D3)}$$

$$\dot{B}_1=-[\delta+\dot{\theta}(t)(\xi+\alpha_-^2-1)]B_2-\dot{\theta}(t)A_2,$$

$$\dot{B}_2=[\delta+\dot{\theta}(t)(\xi+\alpha_-^2-1)]B_1+\dot{\theta}(t)A_1.$$

Initial conditions for Eqs. (D3) at $t=-\infty$ are $A_1=1/\alpha_-$, $A_2=B_1=B_2=0$. The first two equations from the set (D3) are satisfied if

$$A_1(t)=F_1(\delta)[\cos\theta(t)-1]+\alpha_-^{-1},$$

$$A_2(t)=F_2(\delta)[\cos\theta(t)-1], \quad \text{(D4)}$$

$$B_2(t)=F_1(\delta)\sin\theta(t), \quad B_1(t)=-F_2(\delta)\sin\theta(t),$$

where $F_{1,2}(\delta)$ are the factors that have to be determined. Considering the stationary case and inserting $A_{1,2}$ and $B_{1,2}$ into the set (D3) we find that the second two equations from this set turn to be

$$0=-[\delta+\dot{\theta}(t)(\xi+\alpha_-^2-1)]F_1(\delta)\sin\theta(t)+\dot{\theta}(t)F_2(\delta),$$

$$0=-[\delta+\dot{\theta}(t)(\xi+\alpha_-^2-1)]F_2(\delta)\sin\theta(t)+\dot{\theta}(t)[1/\alpha_- -F_1(\delta)]. \quad \text{(D5)}$$

These two equations are identical if

$$\tau\delta\equiv F_2(\delta)/F_1(\delta)=[1/\alpha_- -F_1(\delta)]/F_2(\delta), \quad \text{(D6)}$$

where τ is the pulse duration, so that when $\tau\delta$ is given by Eq. (D6), Eqs. (D5) are equivalent to

$$\dot{\theta}(t)=\frac{\delta\sin\theta(t)}{\tau\delta-(\xi+\alpha_-^2-1)\sin\theta(t)}. \quad \text{(D7)}$$

We integrate Eq. (D7) by separating variables,

$$d\theta\left[\frac{1}{\sin\theta(t)}-\frac{\xi+\alpha_-^2-1}{\tau\delta}\right]=\frac{dt}{\tau}. \quad \text{(D8)}$$

Integration of Eq. (D8) leads to the following equation for $\theta(t)$:

$$\ln\left[\tan\frac{\theta(t)}{2}\right]-\frac{\theta(t)}{\tau\delta}\left(\frac{2\Delta_{d\text{-}d}\Delta_1}{\Omega_{trap}^2}+\alpha_-^2-1\right)=\frac{t-t_0}{\tau}, \quad \text{(D9)}$$

where t_0 is the integration constant. From Eqs. (D6) one can find

$$F_1(\delta)=\frac{1}{\alpha_-[1+(\tau\delta)^2]}, \quad F_2(\delta)=\frac{\tau\delta}{\alpha_-[1+(\tau\delta)^2]}.$$

Inserting these expressions into Eqs. (D4) one can obtain the result (42).

[1] C. A. Sackett *et al.*, Nature (London) **404**, 256 (2000).
[2] A. Steane *et al.*, Phys. Rev. A **62**, 042305 (2000).
[3] H. Walther, Proc. R. Soc. London, Ser. A **454**, 431 (1998).
[4] A. Rauschenbeutel *et al.*, Phys. Rev. Lett. **83**, 5166 (1999).
[5] T. Calarco, H. J. Briegel, D. Jaksch, J. I. Cirac, and P. Zoller, J. Mod. Opt. **47**, 2137 (2000).
[6] G. K. Brennen, I. H. Deutsch, and P. S. Jessen, Phys. Rev. A **61**, 062309 (2000).
[7] N. Schlosser, G. Reymond, I. Protsenko, and Ph. Grangier, Nature (London) **411**, 1024 (2001).
[8] T. Calarco *et al.*, Phys. Rev. A **61**, 022304 (2000); D. Jaksch, H.-J. Briegel, J. I. Cirac, C. W. Gardiner, and P. Zoller, Phys. Rev. Lett. **82**, 1975 (1999).
[9] G. K. Brennen, C. M. Caves, P. S. Jessen, and I. H. Deutsch, Phys. Rev. Lett. **82**, 1060 (1999).
[10] D. Jaksch *et al.*, Phys. Rev. Lett. **85**, 2208 (2000).
[11] D. Frese *et al.*, Phys. Rev. Lett. **85**, 3777 (2000).
[12] M. Morinaga, I. Bouchoule, J. C. Karam, and C. Salomon,

Phys. Rev. Lett. **83**, 4037 (1999).
[13] D. P. DiVincenzo, Phys. Rev. A **51**, 1015 (1995).
[14] R. Feynman, Int. J. Theor. Phys. **21**, 467 (1982).
[15] G. K. Brennen, C. M. Caves, P. S. Jessen, and I. H. Deutsch, Phys. Rev. Lett. **82**, 1060 (1999).
[16] W. R. Anderson, J. R. Veale, and T. F. Gallagher, Phys. Rev. Lett. **80**, 249 (1998).
[17] S. Liberman and J. Pinard, Phys. Rev. A **20**, 507 (1979).
[18] C. E. Moore, *Atomic Energy Levels* (Natl. Bur. Stand., U.S., GPO, Washington, D.C., 1949).
[19] The spontaneous emission lifetime in the presence of $n_T = (e^{\hbar\omega/KT}-1)^{-1}$ thermal photons is $\tau_{sp}/(1+n_T)$. For the transitions between Rydberg states considered here, $\omega \approx 2$ cm^{-1} so that $n_T > 1$ at $T > 4$ K.
[20] P. W. Milonni and P. L. Knight, Phys. Rev. A **10**, 1096 (1974).
[21] M. D. Lukin, M. Fleischhauer, R. Côte, L. M. Duan, D. Jaksch, J. I. Cirac, and P. Zoller, Phys. Rev. Lett. **87**, 037901 (2001).
[22] S. Osnaghi, P. Bertet, A. Auffeves, P. Maioli, M. Brune, J. M. Raimond, and S. Haroche, Phys. Rev. Lett. **87**, 037902 (2001).
[23] I. I. Sobelman, *Introduction to the Theory of Atomic Spectra* (Nauka, Moscow, 1977).
[24] D. R. Bates and A. Damgaard, Philos. Trans. R. Soc. London, Ser. A **242**, 101 (1949).
[25] A. Lindgard and S. E. Nielsen, At. Data Nucl. Data Tables **19**, 606 (1977).
[26] C. Fabre, thèse de doctorat d état, Université Paris 6, 1980.
[27] J. Picart, A. Emonds, Tranh Minh, and R. Rullen, J. Phys. B **11**, L-651 (1978).
[28] G. Peach, Mem. R. Astron. Soc. **71**, 13 (1967).